Numerical Mdel of Riverbank Erosion and Free Meandering

Yasuyuki SHIMIZU[1]

Abstruct

A numerical model is proposed to investigate free meandering of river. Flow field, bed deformation, bank erosion and channel migration are calculated numerically with a general non-orthogonal coordinate system which can be applied to moving boundary conditions. Flow field is calculated from two dimensional momentum equations and continuity equation. Bed deformation is calculated from continuity equation of bed load transport. Bank erosion and deposition is estimated from critical slope of bank material and emergence of bed due to the bed deposition. Time dependent change of channel geometry is calculated with an iteration process of these procedures. Calculated results are favorably compared with experimental results with movable bed and bank, and thus the accuracy of new model is verified.

1. Introduction

Determining the erosion of riverbeds and riverbanks quantitatively is important subject in disaster prevention works. The riverbed erosion in a fixed bank (experimental flumes, rivers with bank protection works, etc.) have been studied on theoretical and experimental bases and numerical models have been developed. As a result, the mechanism of river bed forms has been explained, and numerical models are being established (Shimizu et al. 1995). Studies on bank erosion and river meandering are also being made theoretically and experimentally from various viewpoints, making it possible to understand these events to some extent(Hasegawa 1978; Parker 1983).

The changes in the bed topography and the erosion of banks are not events that occur independently; both of them take place interdependently through water flow and sediment. In designing a model for such events, particularly for natural rivers where banks are not protected, a model is required that can deal with riverbed evolution and bank erosion simultaneously. From this point of view, this study aimed to develop such a model. As a first step toward this aim, this paper describes the development of a model for a river channel whose bed and banks consist of sandy soil. The basis of the model was the computation of a two-dimensional flow and of the bed deformation. In making these computations, general coordinates, enabling a description of a boundary shape that takes an arbitrary form, was used assuming that erosion and sediment deposition occur in the cross-sectional direction to transform the plane shape of the water channel into an arbitrary shape. It is also assumed that the erosion of banks occurs when the gradient in the cross-sectional direction of the banks is steeper than the submerged angle of repose, because of changes in the riverbed erosion near the banks. In this case, the amount of sediment beyond the submerged critical angle of slope is included in the computation of the bankbed evolution, as a supply of sediment from the banks. On the other hand, the inner banks at channel bends and other parts, which were transformed into land while the computing was in process, were successively excluded from the range of computation.

The computational model was verified by conducting model experiments on free meandering. The experimental results showed that the model was effective in simulating precisely the erosion of banks and the changes in the riverbed, i.e., the changes in free meandering through time. The model also proved to be able to quantitatively analyze the free meandering of a river channel.

[1] Associate Professor, Hokkaido University, Japan: yasu@civil.hokudai.ac.jp

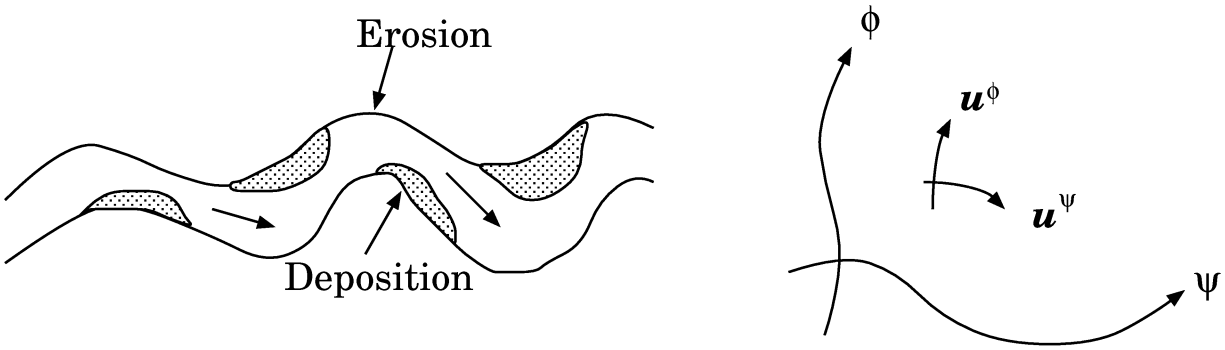

Figure 1: A skech of free meandering channel and definition of general coordinates

2. Framework of the Computational Model

A water channel is defined in this paper as a channel whose width changes by erosion and sediment deposition. For this reason, computation was made by using general coordinates applicable to arbitrary shapes of the channel (Figure 1). The computational model uses the following process, and it calculates the changes in flow and the shape of a channel with time at infinitesimal intervals up to the designated time under the given initial conditions. The subject of the model in this paper is a channel with a flow having a relatively large ratio between the width of the channel and the depth, and that can be approximated to a two-dimensional plane. The same material is assumed for a riverbed and riverbanks.

1. Computing the depth averaged flow field in the given plane shape of a water channel
2. Computing the secondary flow perpendicular to the streamline of the depth averaged flow
3. Computing the sediment transport rate and riverbed evolution
4. The bank erosion, sediment deposition and shape alteration of a channel
5. Setting a coordinate system along a new boundary and updating the computational data
6. Updating time (t=$t + \Delta t$)

3. Computation of Flow and Riverbed Evolution in General Coordinates

Equations of continuity and motion of a two-dimensional shallow water flow in the co-orthogonal coordinates (x, y) are represented as follows:

$$\frac{\partial(hu^x)}{\partial x} + \frac{\partial(hu^y)}{\partial y} = 0 \tag{1}$$

$$\frac{\partial(u^x)^2}{\partial x} + \frac{\partial(u^x u^y)}{\partial y} = -g\frac{\partial H}{\partial x} - \frac{\tau_{bx}}{\rho h} + \frac{\partial}{\partial x}\left(\varepsilon\frac{\partial u^x}{\partial x}\right) + \frac{\partial}{\partial y}\left(\varepsilon\frac{\partial u^x}{\partial y}\right) \tag{2}$$

$$\frac{\partial(u^x u^y)}{\partial x} + \frac{\partial(u^y)^2}{\partial y} = -g\frac{\partial H}{\partial y} - \frac{\tau_{by}}{\rho h} + \frac{\partial}{\partial x}\left(\varepsilon\frac{\partial u^y}{\partial x}\right) + \frac{\partial}{\partial y}\left(\varepsilon\frac{\partial u^y}{\partial y}\right) \tag{3}$$

where x and y are coordinate axes in the co-orthogonal coordinates, u^x and u^y are components of x- and y-directions of velocity, H is the water surface elevation, h is the water depth, g is the acceleration of gravity, ρ is the density of water, ε is the coefficient of eddy viscosity, and τ_{bx} and τ_{by} are the components of the x- and y-directions of bed shear stress. τ_{bx}, τ_{by} and ε are represented by the following equations:

$$\tau_{bx} = \rho C_f u^x\sqrt{(u^x)^2 + (u^y)^2}, \qquad \tau_{by} = \rho C_f u^y\sqrt{(u^x)^2 + (u^y)^2}, \qquad \varepsilon = \frac{\kappa}{6}u_* h \tag{4}$$

where C_f is the friction coefficient of the riverbed, u_* is the shear velocity ($C_f\sqrt{(u_x)^2+(u_y)^2}$), and κ is Karman's universal constant. Eqs. (1)–(3) for the x and y coordinates are transformed into the (ψ,ϕ) coordinates (Fig. 1) by using the following relation:

$$\frac{\partial}{\partial x}=\psi_x\frac{\partial}{\partial \psi}+\phi_x\frac{\partial}{\partial \phi},\qquad \frac{\partial}{\partial y}=\psi_y\frac{\partial}{\partial \psi}+\phi_y\frac{\partial}{\partial \phi} \tag{5}$$

$$u^x=\frac{1}{J}\left(\phi_y u^\psi-\psi_y u^\phi\right),\qquad u^y=\frac{1}{J}\left(-\phi_x u^\psi+\psi_x u^\phi\right),\qquad u^\psi=u^x\psi_x+u^y\psi_y,\qquad u^\phi=u^x\phi_x+u^y\phi_y \tag{6}$$

where $\psi_x=\partial\psi/\partial x$; $\psi_y=\partial\psi/\partial y$; $\phi_x=\partial\phi/\partial x$; $\phi_y=\partial\phi/\partial y$; u^ψ, u^ϕ are contravariant components of flow velocity in the ψ- and ϕ- directions. Using these relations, the basic equations of flow in the general coordinates are given as follows:

$$\frac{\partial}{\partial \psi}\left(\frac{hu^\psi}{J}\right)+\frac{\partial}{\partial \phi}\left(\frac{hu^\phi}{J}\right)=0 \tag{7}$$

$$\begin{aligned}&\psi_x\left\{\frac{\partial}{\partial \psi}\left[\frac{1}{J^2}\left(\phi_y u^\psi-\psi_y u^\phi\right)u^\psi\right]+\frac{\partial}{\partial \phi}\left[\frac{1}{J^2}\left(\phi_y u^\psi-\psi_y u^\phi\right)u^\phi\right]\right\}\\&+\psi_y\left\{\frac{\partial}{\partial \psi}\left[\frac{1}{J^2}\left(-\phi_x u^\psi+\psi_x u^\phi\right)u^\psi\right]+\frac{\partial}{\partial \phi}\left[\frac{1}{J^2}\left(-\phi_x u^\psi+\psi_x u^\phi\right)u^\phi\right]\right\}\\&=-\frac{g}{J}\left[(\psi_x^2+\psi_y^2)\frac{\partial H}{\partial \psi}+(\psi_x\phi_x+\psi_y\phi_y)\frac{\partial H}{\partial \phi}\right]-\frac{\rho C_f}{J^2}u^\psi\sqrt{\left(\phi_y u^\psi-\psi_y u^\phi\right)^2+\left(-\phi_x u^\psi+\psi_x u^\phi\right)^2}+D^\psi\end{aligned} \tag{8}$$

$$\begin{aligned}&\phi_x\left\{\frac{\partial}{\partial \psi}\left[\frac{1}{J^2}\left(\phi_y u^\psi-\psi_y u^\phi\right)u^\psi\right]+\frac{\partial}{\partial \phi}\left[\frac{1}{J^2}\left(\phi_y u^\psi-\psi_y u^\phi\right)u^\phi\right]\right\}\\&+\phi_y\left\{\frac{\partial}{\partial \psi}\left[\frac{1}{J^2}\left(-\phi_x u^\psi+\psi_x u^\phi\right)u^\psi\right]+\frac{\partial}{\partial \phi}\left[\frac{1}{J^2}\left(-\phi_x u^\psi+\psi_x u^\phi\right)u^\phi\right]\right\}\\&=-\frac{g}{J}\left[(\psi_x\phi_x+\psi_y\phi_y)\frac{\partial H}{\partial \psi}+(\phi_x^2+\phi_y^2)\frac{\partial H}{\partial \phi}\right]-\frac{\rho C_f}{J^2}u^\phi\sqrt{\left(\phi_y u^\psi-\psi_y u^\phi\right)^2+\left(-\phi_x u^\psi+\psi_x u^\phi\right)^2}+D^\phi\end{aligned} \tag{9}$$

where J is the Jacobian of the coordinate transformation ($=\phi_y\psi_x-\psi_y\phi_x$). D^ψ and D^ϕ are momentum diffusion terms in ψ- and ϕ- directions of the equation of motion (Shimizu and Itakura 1991).

The continuity equation of two-dimensional bedload transport is represented by the following equation:

$$\frac{1-\lambda}{J}\frac{\partial \eta}{\partial t}+\frac{\partial}{\partial \psi}\left(\frac{q^\psi}{J}\right)+\frac{\partial}{\partial \phi}\left(\frac{q^\phi}{J}\right)=0 \tag{10}$$

where η is the riverbed elevation ($=H-h$), t is time, λ is porosity of bed material. q_ϕ and q_ϕ are the contravariant components of the bedload transport rate per unit width in the ψ- and ϕ- directions, and are expressed by assigning s to the direction of the streamline and n to the direction perpendicular to the streamline:

$$q^\psi=\frac{\partial \psi}{\partial s}q^s+\frac{\partial \psi}{\partial n}q^n=\left(\psi_x\frac{\partial x}{\partial s}+\psi_y\frac{\partial y}{\partial s}\right)q^s+\left(\psi_x\frac{\partial x}{\partial n}+\psi_y\frac{\partial y}{\partial n}\right)q^n \tag{11}$$

$$q^\phi=\frac{\partial \phi}{\partial s}q^s+\frac{\partial \phi}{\partial n}q^n=\left(\phi_x\frac{\partial x}{\partial s}+\phi_y\frac{\partial y}{\partial s}\right)q^s+\left(\phi_x\frac{\partial x}{\partial n}+\phi_y\frac{\partial y}{\partial n}\right)q^n \tag{12}$$

From the direction of the local flow, the partial differential of the s- and n-directions of x and y are expressed as follows:

$$\frac{\partial x}{\partial s}=\frac{u^x}{V},\qquad \frac{\partial x}{\partial n}=-\frac{u^y}{V},\qquad \frac{\partial y}{\partial s}=\frac{u^y}{V},\qquad \frac{\partial y}{\partial n}=\frac{u^x}{V} \tag{13}$$

where $V = \sqrt{(u^x)^2 + (u^y)^2}$. By using these expressions of relation, q^ψ and q^ϕ are expressed as follows:

$$q^\psi = \left(\psi_x \frac{u^x}{V} + \psi_y \frac{u^y}{V}\right) q^s + \left(-\psi_x \frac{u^y}{V} + \psi_y \frac{u^x}{V}\right) q^n = \frac{1}{V}\left(u^\psi q^s - J u_\phi q^n\right) \tag{14}$$

$$q^\phi = \left(\phi_x \frac{u^x}{V} + \phi_y \frac{u^y}{V}\right) q^s + \left(-\phi_x \frac{u^y}{V} + \phi_y \frac{u^x}{V}\right) q^n = \frac{1}{V}\left(u^\phi q^s - J u_\psi q^n\right) \tag{15}$$

where u_ψ and u_ϕ are the covariant components of depth averaged flow velocites in the ψ- and ϕ-directions and are expressed by the following equation:

$$u_\psi = \frac{1}{J}(\phi_y u^x - \phi_x u^y), \qquad u_\phi = \frac{1}{J}(-\psi_y u^x + \psi_x u^y) \tag{16}$$

Meyer-Peter-Müller formula is used for the bed load transport rate :

$$q^s = 8\sqrt{\left(\frac{\rho_s}{\rho - 1}\right) g d^3}(\tau_* - \tau_{*c})^{3/2} \tag{17}$$

where ρ_s is the density of bed material, d is the grain size of bed material, τ_* is the non-dimensional bed shear stress ($= u_*^2/[(\rho_s/\rho - 1)gd]$), and τ_c is the critical non-dimensional bed shear stress obtained by using Iwagaki's equation.

The s-axis is the direction of the streamline arising from the depth averaged flow. Consequently, depth averaged flow in the direction of the n-axis paependicular to the s-axis is zero, and the sediment transport rate in the n-axis direction is also zero. However, a streamline is generally curved along the shape of the channel; when a streamline forms a curve, a secondary flow (spiral flow) is generated. Since this secondary flow is very important for riverbed evolution and the erosion of the banks, its influence must be taken into consideration. Here, equation (18), proposed by Hasegawa (1983), is used to calculate the amount of sediment (q_n) in a direction orthogonal to the streamline, considering the influence of the secondary flow.

$$q^n = q^s \left(\frac{h}{r} N_* - \sqrt{\frac{\tau_*}{\mu_s \mu_k}} \frac{\partial \eta}{\partial n}\right) \tag{18}$$

where r is the radius of curvature of a streamline, N_* is the coefficient of strength of secondary flow, μ_s is the static friction coefficient of sand grain, μ_k is the kinetic friction coefficient of sand grain. In the analysis below, the constants of $N_* = 7.0$ given by Engelund (1974) was used, while mu_s and μ_k are set to 1.0 and 0.45, considering the properties of sand.

In the (ψ,ϕ) coordinate system, r and $\partial\eta/\partial n$ are descrived as:

$$\frac{1}{r} = \frac{1}{V^3}\left[u^\psi\left(\frac{\partial u^y}{\partial \psi} u^x - \frac{\partial u^x}{\partial \psi} u^y\right) + u^\phi\left(\frac{\partial u^y}{\partial \phi} u^x - \frac{\partial u^x}{\partial \phi} u^y\right)\right], \qquad \frac{\partial \eta}{\partial n} = \frac{J}{V}\left(u_\psi \frac{\partial \eta}{\partial \phi} - u_\phi \frac{\partial \eta}{\partial \psi}\right) \tag{19}$$

4. Computations of Channel Deformation

A ψ-axis is drawn along the channel for the given initial plane shape of the channel, and a ϕ-axis is drawn to intersect with the ψ-axis. Then the plane (ψ, ϕ) is properly divided into parts to make the initial grids for the computations. The computations for the flow and the bed evolution are conducted by the finite difference method (Shimizu and Itakura 199?) with these computational grids, for which the equations in Section 3 are used. With special attention on the bed evolutions near the banks, the deformation in the plane shape of the channel are calculated according to the following procedure.

When the computations show that the riverbed near the banks decreases in height, and when the cross-sectional gradient of the bank slope becomes steeper than the submerged angle of repose (θ_c), the result (Figure 2-(A)), as in the study by Hasegawa (1983), is that the sediment beyond the submerged

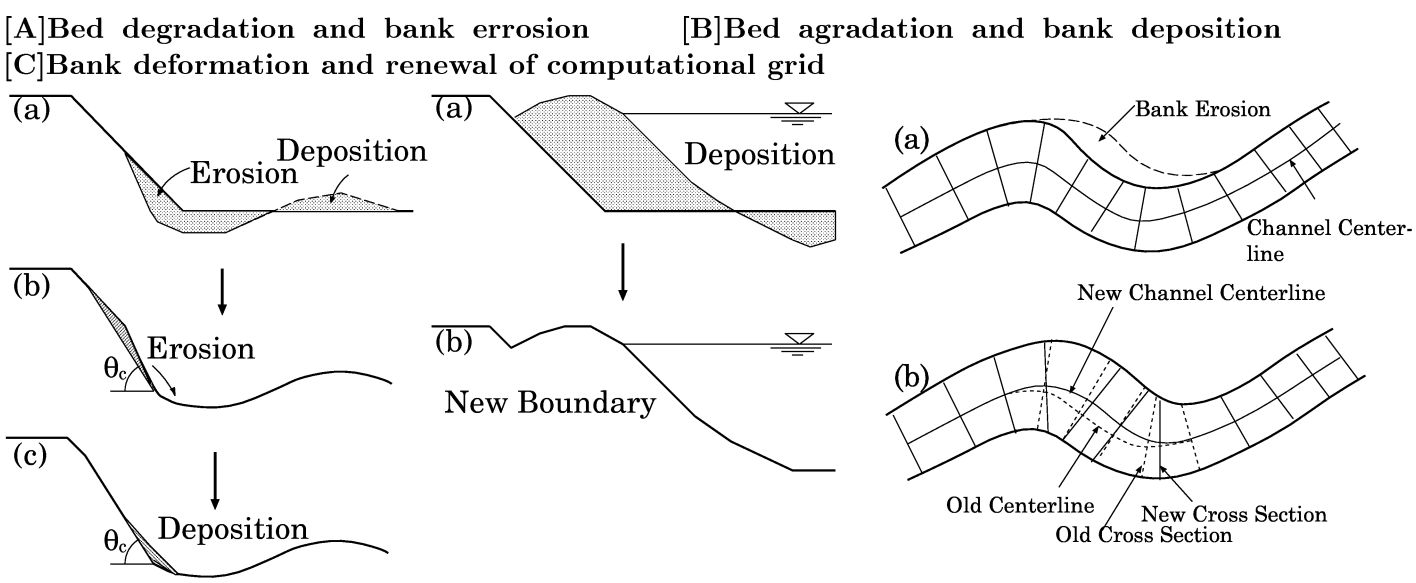

Figure 2: Bed deformation and renewal of channel geometry

angle of repose is assumed to be momentarily eroded to the point of the submerged angle of repose, and then sediment equal to the amount of sediment beyond the submerged angle of repose is deposited at the foot of the bank slope. At this time, if the erosion of the bank slope face advances toward the top of the slope, the computational range is enlarged in the cross-sectional direction of the channel. Moreover, if part of the bed near the banks is transformed into land, narrowing the water channel, the computational range is moved to the new waterline (Figure 2-(B)). When the computational range is enlarged, for example, due to the erosion of the banks (Figure 2-(C)a), (Figure 2-(C)b), (1) a new central line of the channel passing through the center of new banklines is set. (2) Along this new central line of the channel, new cross-sections perpendicular to this line are set at equal intervals as the initial condition in the ψ- direction. (3) Each cross-section is divided into the grid numbers in the ϕ- direction. Thus, new computational meshes are formed, and the computational data are all transformed from old to new computational grid. When transforming all the computational data between the new and old grid, a linear transformation based on geometric locations must be carried out. These calculations are conducted at intervals of a infinitesimal time (Δt) and are continued up to designated time.

5. Comparison with the Experimental Results

In the experiments, a platform with a movable slope of 25m and a width of 3m was used. Its top was covered with Silica Sand No. 5 (average grain size: 0.494 mm, specific gravity: 2.646) of about 17 cm thick. The original shape of the channel was provided with a sine-generated curve with a meandering wave length of 472cm and a meandering angle of 28.7 degree. For the sectional form, trapezoid gutters were cut to flow a given discharge.

Two experiments were carried out under the initial conditions that the non-dimensional channel width (channel width/average water depth) corresponded to (1) the conditions for alternate bars and (2) a no bars, according to the results of a series of experiments on meandering channels with fixed bank and a movable bed conducted by Toyabe, et al. (1993). The conditions, including the discharge, the gradient and the initial cross-sectional form, which conformed to the conditions stated above in this section were set on a trial basis after preliminary experiments, because the erosion of the banks occurred immediately after water flowed into the channel in the experiments. Table 1 shows the initial conditions of the experiments. During the experiments, if necessary, water flow was stopped and drained to measure the changes in the sectional form and the shape of the channel.

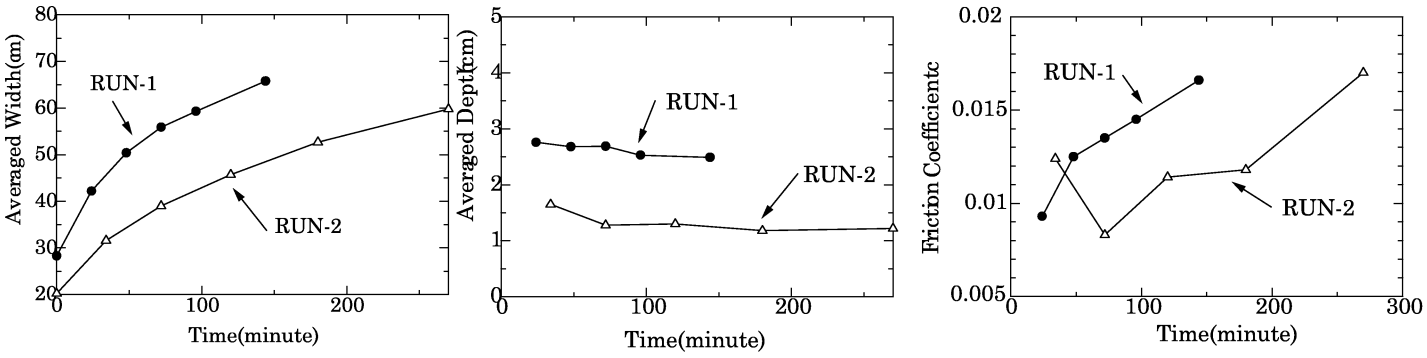

Figure 3: Chanage of averaged width, depth, and friction coefficient C_f

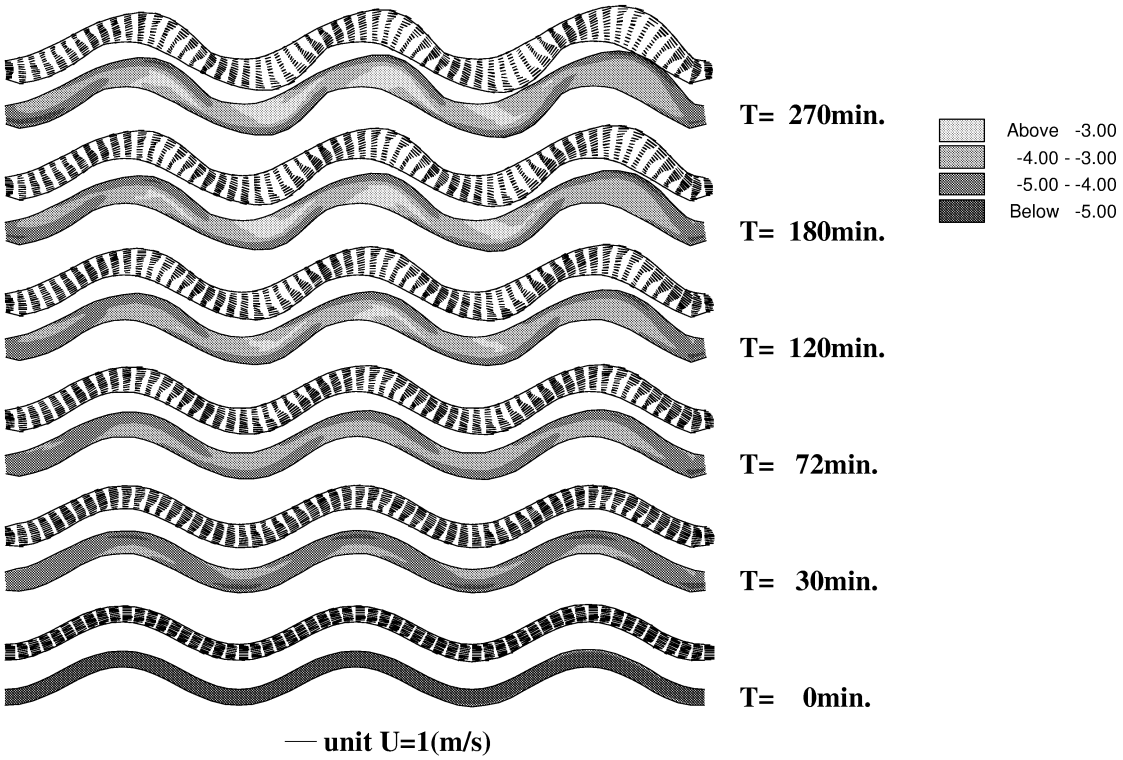

Figure 4: Calculated bed contour and depth-averaged velocity vectors

In both experiments, immediately after the experiment was started, the channel width and the meandering increased, accompanying the erosion of the banks mainly on the downstream side of the outer banks of the meanders. Figs. 3-(a) and (b) show the changes in the average channel width (width of water surface) and the average water depth with time in both experiments. Irrespective of a fixed discharge, the channel width increased three times of that of the beginning of the experiments, but the decrease in water depth was slight, because the friction coefficient increased with the increase in the width of the channel (Fig. 3-(C)). Also, ripples tended to increase on the bed of the experimental channel. Both experiments were ended when the water overflowed the banks in about 150 minutes for Run-1 and in about 270 minutes for Run-2, with an increase in resistance.

The computations were made under the same conditions as the experiments. Figs. 4–6 show the results from the experiments conducted under the conditions of Run-2. Fig. 4 shows the changes in the bed and the vector of the depth averaged flow velocity with time in the contour map. Fig. 5 compares the results of the experiments on the shape of the channel changing with time with the computational results. Fig. 6 compares the results of the experiments of the cross-sectional forms

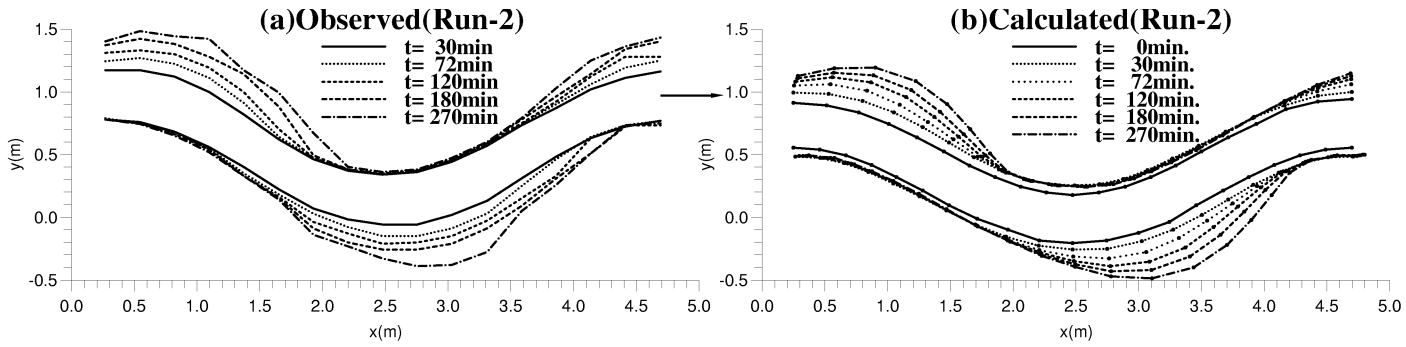

Figure 5: Comparison of channel geometories between calculated and experiment

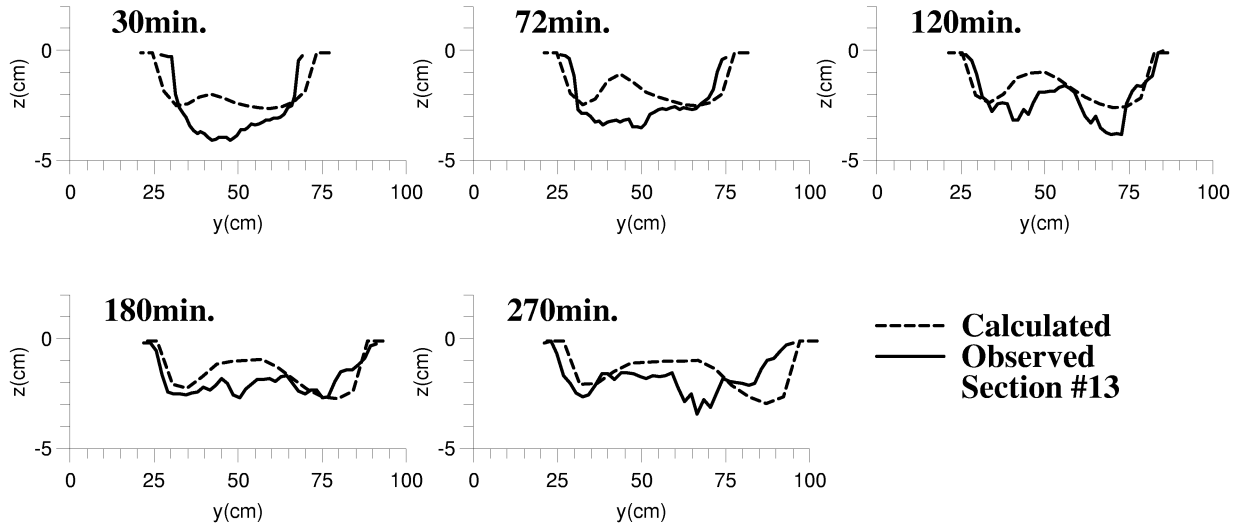

Figure 6: Comparison of channel cross sections between calculated and experiments

corresponding to the initial inflection point in the original shape of the channel with the computational results. The ranges in the contour maps of the plane shape (Fig. 4) and the cahnnel bed (Fig. 5) are those of the width of the water surface. The values on the contour map diagram of the riverbed (Fig. 5) and the ordinate axis (Fig. 6) represent the riverbed height (cm), with the top of the bank slope in the initial stage of the experiments used as a base.

The experimental results show that the erosion of the banks developed near the inflection point centering on the outer banks giving the appearance of the meandering advancing downstream. The cross-sectional form of the channel bed was generally level. In the experiments on fixed banks (Toyabe et al. 1993) conducted under the same hydraulic conditions, deep scouring about twice as deep as the water depth was recorded at the outer banks. On the other hand, in these experiments, the extent of scouring was as deep as the water depth at its maximum. In the latter half of the experiments, the flow separated into two flows with the increase in the width. Thus, sand banks tended to form. The computational results well-simulated the observed condition in the experiments, and thus the numerical computation model seems effective.

6. Conclusion

As a first step to develop numerical computation models capable of dealing with changes in riverbed and riverbanks simultaneously, a model was made to deal with a case where bed and banks consist of sandy soil. A coordinate system was used for the computation in which the boundary can take arbitrary forms. This was because we assumed that erosion and sediment deposition occur laterally, thereby transforming the shape of a channel into arbitrary shapes. The erosion of banks was also

assumed to occur when the gradient in the cross-sectional direction of the bank becomes steeper than a submerged angle of repose, due to the changes in bed topography near the banks. In this case, the amount of sediment beyond the submerged angle of repose was included in the computation of the riverbed evolution as a supply of sediment from the banks. At the same time, inner banks at the channel bends and other parts that were changed into land in the process of the computations were excluded from the range of computation. The model was verified by experiments on free meandering. As a result, the model was proved to be effective for simulating precisely the changes in free meandering accompanying bank erosion with time recognized in the experiments. This study confirmed that the model can analyze the free meandering of sandy channels quantitatively.

References

Engelund, F. (1974). "Flow and bed topography in channel bends." J. Hyd. Div., ASCE, 100(11), 1631–1648.

Hasegawa, K. (1984). "Hydraulic research on planimetric forms, bed topographies and flow in alluvial rivers." Ph. D. Dissertation, Hokkaido Univ., Sapporo, Japan, 1–184 (in Japanese).

Ikeda, S., Yamasaka, M., and Chiyoda, M. (1987). "Bed topography and sorting in bends." J. Hyd. Div., ASCE, 113(2), 190–206.

Itakura, T., Kishi, T., Mori, A., and Kuroki, M. (1988). "A study on the flow and bed deformation in a channel with abrupt changes of the width." Fundamental Studies of Functions of Rivers, Hokkaido Development Bureau, 51-70 (in Japanese).

Iwagaki, Y. (1956). "Hydrodynamical study on critical tractive force." Proc. JSCE, 41, 1-21 (in Japanese).

Meyer-Peter, E., and Muller, R. (1984). "Formulas for bed load transport." Proc., 2nd Meeting IAHR, Stockholm, 39-64.

Nelson., J. M. (1988). "Mechanics of flow and sediment transport over nonuniform erodible beds." Ph.D. Dissertation, Univ. of Wa., 1-227.

Smith, J., and Mclean, S. (1984). "A model for flow in meandering streams." Water Resources Research, 20(9), 1301-1315.

Shimizu, Y., and Itakura, T. (1989). "Calculation of bed variation in alluvial channels." J. Hyd. Engrg., ASCE, 115(3), 367-384.

Shimizu, Y., Yamaguchi, H., and Itakura, T. (1990). "Three-dimensional computation of flow and bed deformation." J. Hyd. Engrg., ASCE, 116(9), 1090–1108.

Struiksma, N., Olesen, K.W., Flokstra, C., and DeVriend, H.J. (1985). "Bed deformation in curved alluvial channels." J. Hyd. Res., IAHR, 23(1),57-79.